molecular pharmaceutics

Article

pubs.acs.org/molecularpharmaceutics

Unraveling the Intracellular Efficacy of Dextran-Histidine Polycation as an Efficient Nonviral Gene Delivery System

Jane Joy Thomas, M. R. Rekha,* and Chandra P. Sharma*

Division of Biosurface Technology, Biomedical Technology Wing, Sree Chitra Tirunal Institute for Medical Sciences & Technology, Trivandrum, Kerala, India

Supporting Information

ABSTRACT: In this study, we attempted to elucidate the capability of a natural polymer dextran, by modification with histidine, to be an efficient, safe and promising nucleic acid delivery system in gene therapy. Physicochemical characterizations were performed to get an insight into the derivative. The efficiency of the derivative as a gene delivery vehicle was also studied in depth using fluorescence microscopy. Extensive efforts were made to have a better understanding of the cellular dynamics involved. The derivative proved itself to be 6.7-fold more excelling than PEI in its transfecting capability. Mechanisms underlying cellular internalization, vector unpacking, intranuclear localization and transgene expression were also investigated. The possibility of recruiting intracellular histone to promote the entry of the gene into the nucleus seemed promising. Our findings also explored the links that mediate the correlation between the uptake of the derivative and various endocytic pathways. The results thus obtained reflect the success of the entire journey of the synthesized delivery vehicle.

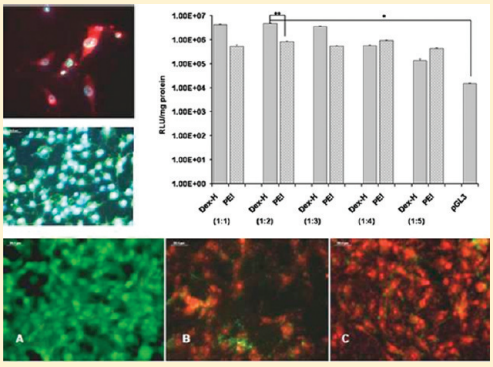

KEYWORDS: *gene delivery, dextran-histidine, histone, intracellular trafficking, p53, vector unpacking*

INTRODUCTION

The fundamental understanding of different genetic disorders led to the progression of gene therapy in various fields like pharmacy, chemistry and medicine. The use of nucleic acids in gene therapy faces various hurdles like large size, negative surface charge, tissue clearance and inefficiency for systemic delivery. A key challenge in addressing the problem in gene therapy lies in the development of specially designed gene delivery systems that are capable of carrying therapeutic genes into mammalian cells for gene expression.[1]

Viruses such as retrovirus and adenovirus are known for their high gene transfer capability. But the use of viral vectors in gene delivery has raised safety concerns based on some adverse dangerous effects which include pathogenicity, immunogenicity, wild type reversion and toxicity.[2]

Nonviral vector mediated gene therapy is currently one of the most attractive alternative strategies used which is free from the risks inherent in viral systems. Various obstacles that limit their use include introduction of plasmid DNA into several cell types and efficient gene expression with limited toxic side effects. Conversely, they offer unique strategies like lower immunogenicity, biocompatibility, safety profiles, biodegradability, low cost production, lack of mutational potential and lack of pathogenicity.[1,3−6]

Nowadays polymers are greatly focused as nonviral delivery agents as they have reached the efficiencies of viral vectors due to their special abilities. Several polymers used in gene delivery include polyethyleneimine (PEI), poly(L-lysine), poly(dimethyl aminoethyl methacrylate) (p(DMAEMA)), poly(trimethyl aminoethyl methacrylate (p(TMAEMA)), poly(vinylpyridine), chitosan, and diethylaminoethyl dextran (DEAE-dextran).[4,5]

Dextrans have been proven to be efficient as nonviral delivery systems.[7] It exhibits several attractive properties like its remarkable degree of biocompatibility, ease of use, biodegradability, availability and improved transfection efficiency with reduced toxicity. It is also easily available, cheap, easily soluble and nontoxic.[8]

The major drawback of native dextran limiting its usage in delivery systems is the high polarity which excludes its transcellular passage. It has been reported that cationized dextran increased transfection efficiency without cytotoxic effects.[9]

Cationic polymers have been promising in neutralizing the anionic nature of DNA thereby efficiently condensing DNA to allow its easy cellular entry.[10] The major problem faced by them is the escape of DNA into the cell cytoplasm from the endosomal compartment for proper gene activity. Therefore a need arises to optimize nonviral vectors to disrupt endosomes and enhance transfection efficiency which generally does not reach adequate therapeutic levels. Certain cationic polymer like poly(L-lysine) does not facilitate the endosomal release of DNA.[11]

The key to the problem of endosomal disruption lies in the use of histidine moieties. Histidine was given importance due to

Received: July 11, 2011
Revised: November 1, 2011
Accepted: November 12, 2011
Published: November 13, 2011

the presence of imidazole in the histidine structure. Imidazole containing polymers is a promising field due to its attractive properties. The biocompatibility of imidazoles[17] helps it to target DNA sequences for alkylating DNA.[13] Reports have stated imidazoles to be antimicrobial[12,16] and also to play a role in the inhibition of cancer proliferation.[12] They were also found to be thermally[14,15] and chemically stable[14,15] and to possess antimetastatic properties.[16] Several studies were done on imidazole and imidazole containing polymers,[16,18,19] but their use in the field of gene therapy is still an unexplored area.

Histidine plays an important role in the disruption of the endosomal membrane by the proton sponge effect of their imidazole groups. The nanoplex after endosomal uptake by the cell has to escape from the endosome to prevent its own lysosomal degradation. This can be made possible based on the hypothesis for endosomal escape called the "proton sponge theory" which focuses on the escape of the nanoplexes from the endosomes by their acidification.[20] The effect protonates the polymer which induces influx of water and ions and endosome destabilization.[21] This brings about large differences in the surface charge of the nanoplex, which leads to structural changes. Disruption of the interaction between the polymer/DNA complex and the endosomal membrane is thus caused.[22] This facilitates the release of the polymer/DNA complex into the cell cytoplasm.[23,24] Histidine moieties are also found to be efficient in improving transfection. The presence of imidazole ring in histidine helps in the enhancement of transfection due to its capability to display a pK_a around 6 and exhibit the proton sponge effect.[25] They were introduced into various polymers to achieve the proton sponge effect without change in the physicochemical properties of the polymer.[25]

The rate limiting steps in gene delivery are endocytosis of the vector, escape from the endosomal compartment, vector unpacking, translocation of DNA into the nucleus and expression of the transgene. With the vision of such a rationale, we synthesized a histidylated dextran derivative (Dex-H) modified with histidine as an endosomolytic agent. The physicochemical properties of Dex-H were characterized. The gene delivery efficiency of the derivative was then evaluated. The effect of histone on the uptake mechanism was also studied. Experiments with fluorescence tags were conducted to investigate the route of polymer/DNA complex internalization in C6 cells and its intracellular processes.

Gene delivery vectors determine their intracellular fate by their route of entry. Several endocytic pathways including caveolae mediated endocytosis, clathrin mediated endocytosis and macropinocytosis play a role in gene uptake. The main aim of this study is to have a better understanding of the intracellular processing and the correlation of each endocytic pathway to the uptake mechanism which opened up possibilities to design a target specific, efficient and safe nucleic acid gene delivery system.

EXPERIMENTAL SECTION

Materials. Dextran (MW 35,600), sodium hydroxide, ethidium bromide (EtBr), 3-(4,5-dimethylthiazol-2-yl)-2,5-diphenyltetrazolium bromide (MTT), Dulbecco's modified Eagle's medium/F-Ham12 (DMEM/F-Ham12), MEM medium, Sephadex G100−120, 0.25% trypsin-ethylenediaminetetraacetic acid (EDTA), amiloride A, histone, nocodazole, cytochalasin B, chlorpromazine, filipin, bafilomycin A_1 and branched PEI (MW 25,000) was purchased from Sigma-Aldrich Chemicals Co., USA. Diamino PEG was from Fluka and L-histidine from SRL. p53 plasmid DNA was from Promega, USA. Deoxyribonucleic acid sodium salt from calf thymus (ctDNA) was from Worthington Biochemical Corp. YOYO iodide and Hoechst 33342 were from Invitrogen. Fetal bovine serum (FBS) was from GIBCO (USA). All other reagents were of analytical grade from Merck, India.

Synthesis of Dextran DAP Histidine (DDH) Conjugates. Dex-H conjugate was synthesized in two steps. In the first step, dextran (MW 35,600 Da) was conjugated with diamino PEG (DAP; MW 1900 Da) by the reductive amination method as described earlier.[26] Oxidized dextran (500 mg) was prepared by reacting dextran in water with sodium metaperiodate at 1:1 mol ratio followed by extensive dialysis against DDW. The dialdehyde dextran solution was then added dropwise to a solution of diamino PEG (200 mg) over 5 h. The reaction mixture was continuously stirred for 24 h at room temperature. The resultant reactant, DDAP, was then purified by extensive dialysis against DDW.

In the second step, histidine moieties were incorporated to 500 mg of DDAP product. A solution of L-histidine (500 mg) was slowly added to the DDAP solution, and the reaction mixture was kept at 25 °C under continuous stirring for 24 h. Varying amounts of L-histidine were also used to modify dextran. The product was recovered by extensive dialysis against double distilled water. The dextran derivative (Dex-H) thus obtained was stored at 4 °C.

PHYSICOCHEMICAL CHARACTERIZATION

Detection of Histidine Moieties. The number of histidine groups on the dextran polymer was spectrophotometrically determination as described elsewhere.[27] Briefly, suitable aliquots of histidine standards and Dex-H of varying concentrations were made up to 1 mL using 1 M NaOH. To 50 μL of the sample, 100 μL of coloring reagent containing sodium nitrate, hydrochloric acid and sulfanilic acid was added and absorbance was read at 405 nm exactly at the 6th min against 1 M NaOH as the blank. Absorbance was plotted against concentration.

Formation of Nanoplexes. A series of nanoplexes of various weight ratios ranging from 1:1 to 6:1 were formulated using Dex-H and calf thymus DNA (ctDNA). Constant amount of ctDNA and varying amounts of Dex-H were separately diluted in saline to a volume of 100 μL. The Dex-H solution was then added to the DNA solution, vortexed and incubated for 30 min at room temperature prior to use. The nanoplexes denoted as DHP were then characterized and used for further cellular studies.

Fourier Transform Infrared Spectroscopy. The test samples of dextran and Dex-H were prepared in a dry powdered form and subjected to FTIR. The spectra obtained were recorded and compared using a Nicolet 5700 spectrophotometer.

Nuclear Magnetic Resonance Spectroscopy. The ^1H NMR spectra of dextran and Dex-H was obtained using NMR spectrometer (Bruker Avance DPX 300). The polymer for study was dissolved in D_2O and analyzed, and spectra were generated for comparison.

Gel Permeation Chromatography. Gel permeation chromatography of Dex-H was performed based on size exclusion using a Sephadex G100−120 column to detect cross-linking of polymers. The column was calibrated using three different molecular weight standards of dextran (Sigma-Aldrich Chemical Co., USA).

Particle Size and Zeta Potential Determination. The mean hydrodynamic sizes of the nanoplexes were characterized by the dynamic light scattering measurement. It was evaluated

using a Zetasizer Nano ZS (Malvern Instruments Ltd., U.K.) at a temperature of 25 °C. The nanoplexes with increasing Dex-H/DNA ratios ranging from 1:1 to 3:1 were allowed to form for 15 min in saline at room temperature. The surface charge of the nanoplexes of varying ratios was also measured using Zetasizer Nano ZS (Malvern Instruments Ltd., U.K.) at a temperature of 25 °C. The zeta potential was calculated using the Smoluchowsky approximation.

Gel Retardation Assay. The efficiency of DNA condensation was assessed by agarose gel electrophoresis. Nanoplexes of desired ratios were prepared with ctDNA and increasing concentration of Dex-H. The stability of the nanoplexes was analyzed on 0.8% agarose gel containing ethidium bromide in Tris-acetate-EDTA (TAE) buffer solution. Electrophoresis was carried out at 100 V for 30 min in a Biorad electrophoresis system (Biorad Laboratories, Hercules, CA, USA). The gel was then photographed and DNA bands were visualized using a MultiImage Light Cabinet (Alpha Innotech Corporation, San Leandro, CA, USA).

Heparin Release Studies. The release of DNA from the nanoplex on treatment with anionic agents like heparin was determined by performing the heparin release studies. Nanoplexes of desired ratios were prepared with ctDNA and increasing concentration of Dex-H. They were then incubated with heparin (0.1 IU/mL) for 30 min at 37 °C. The stability of the nanoplexes was analyzed on 0.8% agarose gel containing ethidium bromide in TAE buffer solution. Electrophoresis was carried out at 100 V for 30 min in a Biorad electrophoresis system (Biorad Laboratories, Hercules, CA, USA). The gel was then photographed and DNA bands were visualized using a MultiImage Light Cabinet (Alpha Innotech Corporation, San Leandro, CA, USA).

Gel retardation studies were also performed in the presence and absence of heparin by complexing Dex-H with p53 plasmid DNA at ratios varying from 1:1 to 6:1.

Acid−Base Titration. The protonating ability of Dex-H was evaluated by acid base titration over a pH range of 10 to 5. Test solutions containing various concentrations of Dex-H were first titrated to pH 10 with 1 N sodium hydroxide. The diluted solutions were then titrated by the sequential addition of 20 μL aliquots of 1 N HCl to a pH of 5. The pH profile was obtained during the titration.

CELL CULTURE STUDIES

Cell culture studies were performed using C6 cells, an adherent fibroblast glioma cell line derived from rat tissue, and HepG2 cells, human liver hepatocellular carcinoma cell line. Cells were cultured in DMEM/Ham's F12:MEM (1:1) medium supplemented with 10% FBS for C6 cells and MEM medium with 10% FBS for HepG2 cells at 37 °C using a humid 5% CO_2 incubator. All experiments were carried out in DMEM/Ham's F12:MEM (1:1) medium supplemented with 10% FBS and MEM medium with 10% FBS respectively.

Cytotoxicity. The evaluation of the viability and proliferation of cells against Dex-H was assayed by the 3-(4,5-dimethylthiazol-2-yl)-2,5-diphenyltetrazolium bromide (MTT) Assay. Prior to assay, both rat fibroblast glioma cell line (C6 cell lines) and human liver hepatocellular carcinoma cell line (HepG2 cell lines) were seeded in multiwell tissue culture plates respectively and cultured at 37 °C, 5% CO_2 atm for 24 h. The cells were then incubated with Dex-H of varying mass concentrations along with PEI as positive control and medium as negative control in triplicate and incubated at 37 °C for 24 h under 5% CO_2 atm. After 24 h of incubation, samples were removed, MTT reagent (0.5 mg/mL) was added to each well and the cells were further incubated for 3 h. The reagent was then removed, and 250 μL of DMSO was added to dissolve the MTT formazan crystals thus formed. Plates were gently agitated at room temperature for 5 min. The results were expressed as the mean % cell viability relative to untreated cells by recording the absorbance of each sample solution at 570 nm using an automated microplate reader (Finstruments Micro plate Reader USA).

Transfection. Before transfection trials, C6 cell lines and HepG2 cell lines were seeded in multiwell plates in culture medium and incubated at 37 °C overnight to get a confluency of 80%. Cells were treated with nanoplexes prepared from ratios 1:1 to 5:1 using Dex-H and pGL-3 plasmid, which was used as the reporter gene. The cells were incubated with the samples for 3 h at 37 °C under 5% CO_2 atmosphere. Later the growth medium was removed; cells were washed with phosphate buffered saline and then cultured further for 48 h. Cells were washed once and then permeabilized for 5 min to harvest cell lysates. The luciferase activity was measured by the addition of the luciferase assay substrate to the supernatant collected. The luciferase gene expression efficiency expressed as RLU (relative light units)/mg of cellular protein was recorded by a luminometer (Chamaleon, Hidex). Total protein was measured using bicinchoninic acid (BCA) protein assay kit (Pierce, USA).

CELLULLAR UPTAKE OF DHP

Plasmid Trafficking Studies. C6 cells were subcultured from the stock culture and seeded into 4 well plates. p53 plasmid was rendered fluorescent by tagging it with a high affinity intercalating fluorescent labeling dye, YOYO iodide, by incubation for 1 h. Nanoplexes were prepared with Dex-H and YOYO tagged plasmid DNA at two different ratios. The cells were incubated with the fluorescent nanoplexes for 3 h at 37 °C in DMEM/Ham's F12:MEM (1:1) medium with 10% FBS. Nuclear staining was performed using Hoechst 33342 by incubation for 1/2 h to assess the nanoplex entry. Later cells were washed with phosphate buffered saline and fixed in 2% formaldehyde. Plasmid trafficking was visualized and photographed using fluorescence microscope (Leica DM IRB, Germany).

Polymer Trafficking Studies. Dex-H was tagged using an amino reactive labeling reagent, TRITC (tetramethylrhodamine isothiocyanate) prepared in DMSO. To a solution of Dex-H (1 mg/mL) was added sodium bicarbonate. TRITC (0.5 mg/mL) was added to the mix and incubated for 2 h at 37 °C. The reaction was stopped by the addition of ammonium chloride. The polymer solution was then dialyzed at 4 °C for 24 h to remove unbound TRITC. Meanwhile, nanoplexes were prepared with both tagged Dex-H and DNA at two different ratios. The cells were incubated with the fluorescent nanoplexes for 3 h at 37 °C. Nuclear staining was performed using Hoechst 33342 by incubation for 1/2 h. The cells were then washed with phosphate buffered saline and fixed in 2% formaldehyde. Polymer trafficking was visualized and photographed using fluorescence microscope (Leica DM IRB, Germany).

Effect of Histone on DHP. C6 cells were subcultured from the stock culture and seeded into 4 well plates. p53 plasmid and Dex-H was rendered fluorescent by tagging it with YOYO iodide and TRITC respectively. Nanoplexes were prepared by incubating polymer and DNA in a fixed ratio for 20 min. After 5 min of incubation, histone of varying concentrations

ranging from 1 ng to 80 μg was added and nanoplexes were further incubated for 15 min. The fluorescent nanoplexes were then added to the cells, and the cells were incubated for 3 h at 37 °C. Nuclear staining was performed using Hoechst 33342 by incubation for 1/2 h. Later cells were washed with phosphate buffered saline and fixed in 2% formaldehyde. Plasmid trafficking was visualized and photographed using fluorescence microscope (Leica DM IRB, Germany).

Live and Dead Assay. C6 cells were seeded into 24 well plates and allowed to adhere overnight with 5% CO_2 at 37 °C. Dex-H and p53 plasmid was used to form nanoplexes in two different ratios. The cells were then incubated with the desired amount of nanoplexes for 3 h. At the end of the incubation period, the medium was replaced with fresh medium and the cells were then incubated for an additional 48 h. The Live and Dead assay was performed using the Live and Dead kit protocol. Prior to the assay, cells were washed thrice with phosphate buffered saline. A 10 mL solution of phosphate buffered saline containing 2 μM calcein AM and 4 μM EthD-1 was prepared and added to the cells, which were further incubated for 30 min at 37 °C. The state of the cells was visualized at the end of 3 h, 24 h and 48 h and photographed using fluorescence microscope (Leica DM IRB, Germany).

EXPLORING THE UPTAKE PATHWAY OF DHP

Cytotoxicity Assay of Inhibitors. The evaluation of the toxicity of cells against various inhibitors was assayed by the 3-(4,5-dimethylthiazol-2-yl)-2,5-diphenyltetrazolium bromide (MTT) assay. Inhibitors used for the study were chlorpromazine (2 μg/mL), to inhibit the formation of clathrin vesicles; filipin (5 μg/mL), to inhibit caveolae mediated endocytosis; nocodazole (7.5 μg/mL), to inhibit microtubule formation; bafilomycin A_1 (200 nM), to inhibit the vacuolar ATPase endosomal proton pump; cytochalasin B (200 μM), actin depolymerizing agent; and amyloride (2.25 μg/mL), which inhibits macropinocytosis by inhibiting the sodium proton exchange. Prior to assay, rat fibroblast glioma cell line (C6 cell lines) was seeded in multiwell tissue culture plates and cultured at 37 °C, 5% CO_2 atm for 24 h. The cells were then incubated with inhibitors of respective concentrations along with PEI as positive control and medium as negative control in triplicate and incubated at 37 °C for 24 h under 5% CO_2 atm. After 24 h of incubation, samples were removed, MTT reagent (0.5 mg/mL) was added to each well and the cells were further incubated for 3 h. The reagent was then removed and 250 μL of DMSO was added to dissolve the MTT formazan crystals thus formed. Plates were gently agitated at room temperature for 5 min. The results were expressed as the mean % cell viability relative to untreated cells by recording the absorbance of each sample solution at 570 nm using an automated microplate reader (Finstruments Micro plate Reader USA). Cytotoxicity assay was also performed with Dex-H in the presence of various inhibitors and expressed as the mean % cell viability relative to untreated cells.

Inhibition Assay by Endocytic Inhibitors. The pathway governing the uptake of Dex-H was determined by the inhibitor study.[28] C6 stable cell lines were pretreated with DMEM/Ham's F12:MEM (1:1) medium containing selective inhibitors of the endocytic pathway for 30 min at 37 °C. Inhibitors used for the study were chlorpromazine (2 μg/mL), to inhibit the formation of clathrin vesicles; filipin (5 μg/mL), to inhibit caveolae mediated endocytosis; nocodazole (7.5 μg/mL), to inhibit microtubule formation; and bafilomycin A_1, to inhibit the vacuolar ATPase endosomal proton pump (200 nM). The inhibitor solution was then removed, and the cells were transfected with nanoplexes of two different ratios containing Dex-H and p53 plasmid for 3 h. Nucleus was stained using Hoechst 33342 by incubating for 1/2 h. The cells were then washed with phosphate buffered saline and fixed using 2% formaldehyde. The effect of the inhibitors was analyzed and photographed using a fluorescence microscope (Leica DM IRB, Germany).

Inhibition Assay by in Vitro Transfection. Transfection inhibition studies were carried out using C6 cell lines which were seeded into 24 well plates and allowed to adhere overnight. They were pretreated with DMEM/Ham's F12:MEM (1:1) medium containing endocytic inhibitors including chlorpromazine (2 μg/mL), to inhibit the formation of clathrin vesicles; filipin (5 μg/mL), to inhibit caveolae mediated endocytosis; and nocodazole (7.5 μg/mL), to inhibit microtubule formation for 30 min at 37 °C. The cells were then transfected with nanoplexes of two different ratios containing Dex-H and p53 plasmid. After 3 h the medium was replaced with fresh medium and the cells were cultivated for 48 h. The luciferase gene expression expressed as RLU (relative light units)/mg of cellular protein was recorded by a luminometer (Chameleon, Hidex), and total cellular protein concentration was measured using bicinchoninic acid (BCA) protein assay kit (Pierce, USA).

Role of Actin and Microtubules. To study the role of microtubules and actin, C6 cells were pretreated with nocodazole (7.5 μg/mL) and its combinations with other inhibitors for 1 h. The cells were then incubated with the prepared nanoplexes containing Dex-H and YOYO tagged p53 plasmid and incubated for 3 h. Nucleus was stained using Hoechst 33342 by incubating for 1/2 h. After incubation, the cells were washed with phosphate buffered saline and fixed using 2% formaldehyde. They were then washed, permeabilized using 0.5% Triton X-100 for 15 min and blocked by 1% BSA. The cells were then incubated in Rhodamine-phalloidin for 15 min. Later the cells were washed thrice with PBS and observed under fluorescence microscope (Leica DM IRB, Germany).

Statistical Analysis. All quantitative data of cell experiments were expressed with error bars which represent the standard deviation (SD). Significance in difference was assessed using Student's t test. P value < 0.05 is considered significant, and P value < 0.001 is considered highly significant.

RESULTS

Synthesis. Cationized dextran derivative was synthesized by incorporating histidine moieties to the dextran polymer. Conjugates of dextran with diamino PEG was prepared by reductive amination. Histidine was then coupled to dextran with the help of the diamino PEG spacer arm. A schematic of Dex-H synthesis and its chemical structure is depicted in Figure 1.

Fourier Transform Infrared Spectroscopy. FTIR analysis was performed to characterize Dex-H. The spectrum of Dex-H depicted strong amide absorbance as new peaks at 1608.9 cm^{-1} and 1451.6 cm^{-1}. Formation of peaks characteristic for imidazole rings at 1091.8 cm^{-1} was also detected (Figure S1 in the Supporting Information).

Nuclear Magnetic Resonance Spectroscopy. The ^1H NMR studies in D_2O was performed to get an insight into the characterization of Dex-H. The NMR spectra of dextran and Dex-H were compared as shown in Figure 2. It showed peaks of

imidazole at 7.61 ppm and 6.92 ppm, of α −CH− peak of histidine at 4.69 ppm and of β −CH_2− peak of histidine at 2.96.

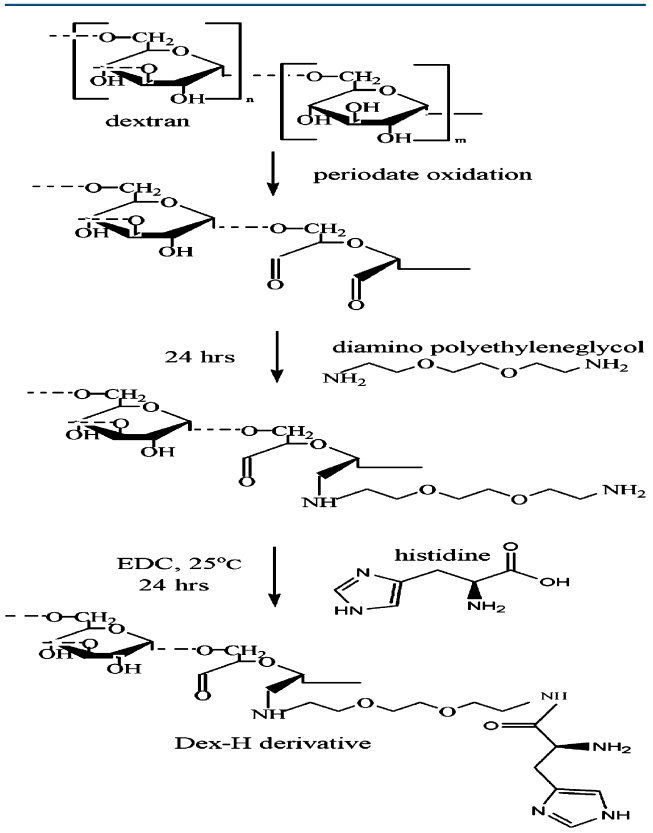

Figure 1. A schematic depicting the synthesis of Dex-H comprising dextran, diamino PEG and histidine.

Detection of Histidine Moieties. The number of histidine groups on the dextran polymer was determined by spectrophotometric analysis. From the calibration curve, 32.4 mg of histidine was found bound to 1 g of dextran.

The molecular weight of dextran used for synthesizing the derivative was 35,600 Da. Gel permeation chromatography analysis reveals the molecular weight of the derivative to be 36,982 Da.

Formation of Nanoplexes: Particle Size and Zeta Potential Determination. Nanoplexes were prepared by the incubation of appropriate concentrations of Dex-H solutions to the standard DNA solution at different Dex-H/DNA weight ratios at 37 °C for 30 min. The measurement of the particle size by dynamic light scattering was performed at 25 °C. A size distribution of 109 to 115 nm was depicted by nanoplexes according to the polymer/DNA weight ratio. The size distribution profile showed no significant difference during the complex formation of the polymer and DNA at different weight ratios.

The surface charge and stability of the nanoplexes was also asserted by the determination of the zeta potential by dynamic light scattering performed at 25 °C. The hydroxyl group of dextran and the phosphate group of DNA affirmed the zeta value of dextran and DNA as −2.84 mV and −14.3 mV respectively. The surface charge of the Dex-H/DNA complexes ranged from +9 mV to +11 mV based on the increase in the weight ratio of Dex-H to DNA (Table 1 in the Supporting Information). The least nanometric size and favorable zeta potential was detected at the ratio 2:1 of Dex-H to DNA.

Gel Retardation Assay. The DNA binding property of Dex-H was assessed by monitoring the electrophoretic mobility of DNA using agarose gel electrophoresis. The electrophoretic gel pattern of Dex-H is shown in Figure 3. It was observed that nanoplexes of higher weight ratios were retained in the agarose wells. Gradual DNA retardation was observed as the concentration of Dex-H in the nanoplex increased. The migration

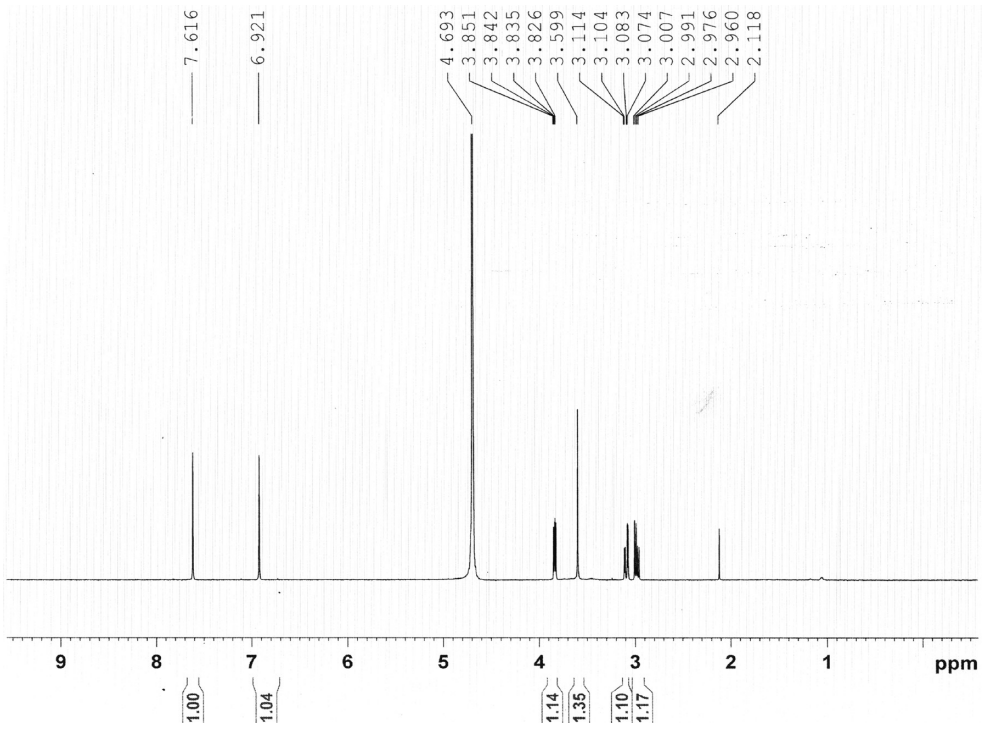

Figure 2. ^{1}H NMR spectra of Dex-H. The NMR spectrum depicts three distinctive peaks characteristic to histidine at 7.61 ppm and 6.92 ppm (imidazole), 4.69 ppm (α −CH− peak) and 2.96 (β −CH_2− peak).

dx.doi.org/10.1021/mp200485b | *Mol. Pharmaceutics* 2012, 9, 121−134

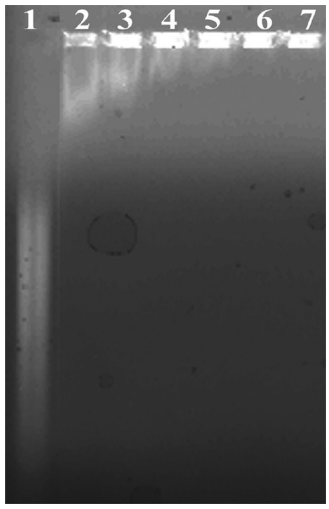

Figure 3. Stability of Dex-H/DNA complexes at different weight ratios detected after 30 min of complexation compared with naked DNA. Lane 1 indicates calf thymus DNA. Lanes 2 to 7 indicate the polymer/DNA complexes at various ratios (0.5:1, 1:1, 1.5:1, 2:1, 3:1 and 4:1).

capability of DNA was found to be completely hindered from ratio 2:1 and above indicating the neutralization of the charge of DNA with that of Dex-H (lanes 2 to 7). A complete retardation assures strong complexation between Dex-H and DNA.

Heparin Release Studies. The release of DNA from the strongly bound nanoplex on treatment with anionic agents like heparin was checked by the heparin release studies. Dex-H/DNA complexes of different ratios (1:1, 2:1, 3:1) were incubated with heparin and then run on 0.8% agarose gel. Naked DNA migrated down (lane 1). On incubation of complexes with heparin, no DNA was detected to be eluted out from the well (lanes 2 to 4) as shown in Figure 4. This proved the strong

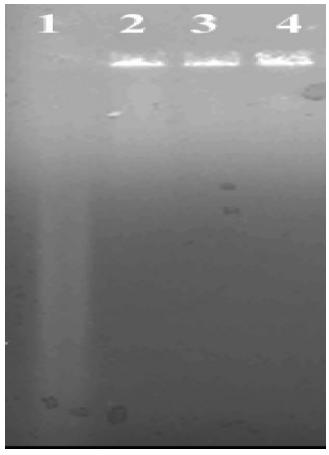

Figure 4. Stability of Dex-H/DNA complexes at different weight ratios detected after 30 min of incubation with heparin compared with naked DNA. Lane 1 indicates calf thymus DNA. Lanes 2 to 4 indicate the polymer/DNA complexes at various ratios. (1:1, 2:1, 3:1).

complexation of DNA with Dex-H, and thus heparin, being an anionic agent, was not able to displace DNA from Dex-H.

Complexes were also prepared in varying ratios and incubated in the presence and absence of heparin where plasmid DNA was used instead of ctDNA for complexation with Dex-H. Here, lane 1 indicates naked plasmid DNA, p53. Lanes 2 to 7 represent complexes of ratios 1:1 to 6:1 in the absence of heparin, and lanes 8 to 13 represent complexes of ratios 1:1 to 1:6 in the presence of heparin (Figure S2 in the Supporting Information). It was detected that strong complexation had taken place between the polymer and the plasmid DNA.

Acid–Base Titration. Acid–base titration of the polymer was performed to study the buffering capability of Dex-H. The buffering capacity versus pH profile of Dex-H and PEI was compared as given in Figure 5. The titration curve trend of

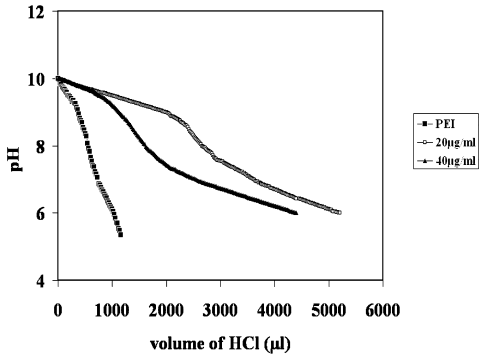

Figure 5. Acid–base titration curves of Dex-H at two different concentrations (20 μg/mL and 40 μg/mL). The solution was titrated with 0.01 N HCl. The titration curve of PEI (1 mg/mL) is given as reference.

Dex-H depicts remarkable buffering capacity over the entire physiological pH range. The pH profile of Dex-H measured at two different concentrations of 20 μg/mL and 40 μg/mL showed a gradual decrease from pH 10 to pH 5. Up to addition of 2000 μL of 0.1 N HCl, no significant change in the pH was detected. The horizontal pH curve trend is ascribed to strong endosomal pH buffering capacity of Dex-H which is due to the presence of imidazole and α amine of histidine.

Cytotoxicity. In cytotoxicity assay, the % viability of Dex-H in higher concentrations was studied in C6 cells and HepG2 cells respectively. Figure 6 shows the cytotoxicity profiles of

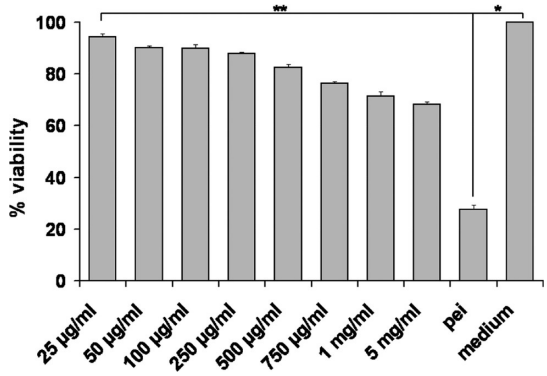

Figure 6. Cytotoxicity of C6 cells after incubation of Dex-H at different concentrations and PEI for 24 h. Cytotoxicity was evaluated by the MTT assay and expressed as % cell viability. Dex-H showed 96.2% at 25 μg/mL and 69.5% (**, P value = 0.034, compared with medium) at 5 mg/mL. Results were expressed as means ± standard deviation. Results were expressed as means ± standard deviation, *, P value < 0.001, compared with medium.

Dex-H in the C6 cell line. The quantitative assessment of cytotoxicity by the MTT assay of cells after contact with the

derivative showed 96.2% metabolically active cells at the lowest concentration and 69.5% (**, P value = 0.034, compared with medium) metabolically active cells at the highest concentration. The viability test proved Dex-H to be the least toxic polymer on comparison with PEI, taken as the positive control in terms of cell toxicity.

Cytotoxicity was also performed in human cell strain, HepG2 cell line. Figure 7 shows the cytotoxicity profiles of Dex-H in

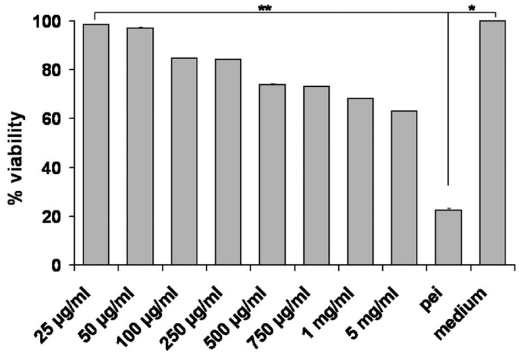

Figure 7. Cytotoxicity of HepG2 cells after incubation of Dex-H at different concentrations and PEI for 24 h. Cytotoxicity was evaluated by the MTT assay and expressed as % cell viability. Dex-H showed 98.51% at 25 μg/mL and 63.1% (**, P value = 0.19, compared with medium) at 5 mg/mL. Results were expressed as means ± standard deviation. Results were expressed as means ± standard deviation, *, P value < 0.001, compared with medium.

the HepG2 cell line. Here, cell viability of Dex-H was detected until a higher concentration of 5 mg/mL. The percent cell viability of Dex-H at the lowest concentration of 25 μg/mL was estimated as 98.5% and at the highest concentration of 5 mg/mL as 63.1% (**, P value = 0.19, compared with medium).

Even at a higher concentration of 5 mg/mL, cytotoxicity was seen to be low in both the cell lines. More than 60% of the cells were viable in the entire concentration range from 25 μg/mL to 5 mg/mL when performed in two different cell lines proving Dex-H to be a nontoxic derivative suitable for gene delivery. Results were expressed as means ± standard deviation, *, P value < 0.001, compared with medium.

Transfection. Transfection was performed in C6 cells using Dex-H and pGL3 plasmid DNA complexed in various weight ratios. The transfection efficiency of Dex-H along with PEI of various weight ratios of 1:1 and 1:5 in the presence of 10% FBS was analyzed by the luciferase activity assay as in Figure 8. The level of luciferase expression due to the presence of Dex-H in the first three ratios (1:1 to 1:3) was found to be remarkably high in the presence of serum when compared to PEI, taken as control. As the ratio of the complex went higher, transfection efficiency was found to reduce. The transfection efficiency of pGL3 plasmid alone was also found to be low. The derivative at ratio 1:2 proved itself to be 6.7-fold more excelling than PEI in its transfecting capability. Results were expressed as means ± standard deviation, *, P value < 0.001, compared with plasmid DNA pGL3; **, P value < 0.001, compared with PEI.

Transfection efficiency of Dex-H coupled to DNA in ratios 1:1 to 1:5 was also performed in the HepG2 cell line. The derivative showed a considerable high level of transfection efficiency favorably in HepG2 cells. The high level of gene expression was detected for the lower ratio 1:2 of the Dex-H/DNA complex. As the ratio of the complex went higher,

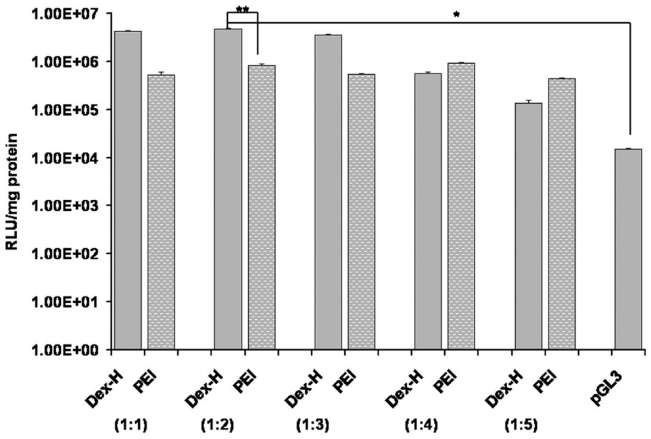

Figure 8. A comparison of the luciferase expression in C6 cells transfected by Dex-H/DNA complexes and PEI/DNA complexes taken at various ratios (1:1 and 5:1). The relative transfection efficiency was tested in the presence of 10% FBS. Results were expressed as means ± standard deviation, *, P value < 0.001, compared with plasmid DNA pGL3; **, P value < 0.001, compared with PEI.

transfection efficiency was found to reduce. The luciferase activity pattern detected in the HepG2 cell line was similar to the C6 cell line data as described above (data not shown).

Plasmid Trafficking Studies. The interpretation of gene transport experiments which mainly rely on the entry of DNA into mammalian cells was examined using fluorescence microscopy. Observations were recorded after 3 h of incubation of C6 cells with Dex-H complexed with DNA tagged using YOYO-I. The uptake of the nanoplex was evaluated by the influx of the fluorescently tagged plasmid DNA depicted in green dots. From Figure 9A, it was seen that high fluorescence

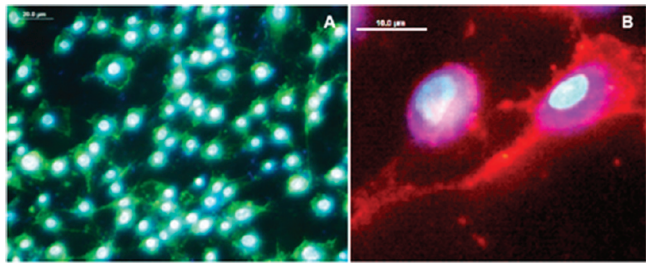

Figure 9. Intracellular distribution of plasmid DNA (A) and Dex-H (B) in C6 cells. Plasmid DNA was tagged with YOYO-I (green), and Dex-H was tagged with TRITC (red). Cells were transfected with Dex-H/DNA complexes of ratio 2:1. Fluorescent microscopic images were taken at a magnification of 40×.

signals from plasmid DNA were found localized in the nucleus along with diffused fluorescence in the cytosolic area. Presence of histidine did not affect the rapid cellular internalization of the nanoplex but helped to increase the nuclear access of DNA.

Polymer Trafficking Studies. Dex-H was tagged with TRITC, complexed with plasmid DNA and transfected to study the intracellular distribution of the polymer within the cell using fluorescence microscopy. The polymer was seen to be distributed within the cytoplasm and at the cell periphery whereas it was not detected in the nucleus. The fluorescence profile of Dex-H exhibited by red dots is depicted in Figure 9B.

Effect of Histone on DHP. The experiment with histones was performed by dual fluorescence labeling. Both polymer and

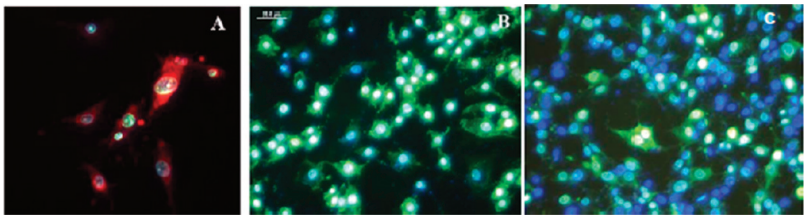

Figure 10. Fluorescent micrographs of the intracellular distribution of Dex-H/DNA complexes in the absence (A) and presence (B) of histone in C6 cells. Plasmid DNA was tagged with YOYO-I (green) and Dex-H was tagged with TRITC (red). Nucleus was stained using Hoechst 33342 (blue). Tagged Dex-H/DNA complexes of ratio 2:1 were incubated with histone for 15 min. Cells were then incubated with the complexes for 3 h at 37 °C. Magnification and scale bar represent 40× and 20 μm respectively.

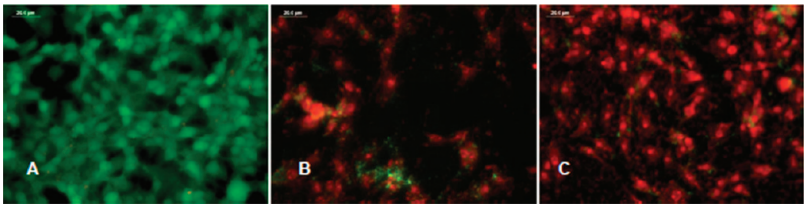

Figure 11. Live/dead assay of C6 cells transfected with DDH/DNA complexes and visualized at each time point of incubation. Cells were incubated with Dex-H complexed with p53 plasmid DNA at 37 °C under 5% CO_2 atm at various time intervals. Cells were examined by fluorescence microscopy at the end of 3 h (A), 24 h (B) and 48 h (C). Green fluorescence depicts live cells, and red fluorescence depicts dead cells. Magnification and scale bar represent 40× and 20 μm respectively.

DNA were labeled and then complexed together in vitro by incubation in the presence and absence of histones respectively. Figure 10 shows the intracellular distribution of TRITC and YOYO-I tagged Dex-H/DNA complexes in the presence and absence of histone.

In the absence of histone, strong fluorescence by Dex-H in the cytoplasmic region and DNA in the nucleus was detected as in Figure 10A. Here, DNA and polymer remained tightly associated until it reached the cytoplasm, and then the DNA was found to be unpacked and transported into the nucleus as detected by YOYO labeling. Here polymer stayed back in the cytoplasm as detected by TRITC labeling. But when the nanoplex was incubated with histones outside the cell, no polymer was detected anywhere in the cell after the cell uptake. Thus in the presence of histone incubation, strong fluorescence by DNA only was detected in both the cytoplasm and the nuclear region. Absence of fluorescence signals from Dex-H is depicted in Figure 10B and Figure 10C. Cellular uptake of DNA into the nucleus was found to be greater in the presence of histone. Histones of varying concentrations ranging from 1 ng to 80 μg were used to determine its vector unpacking capability. Figure 10B depicts histone concentration of 20 μg, and Figure 10C depicts histone concentration of 1 ng. Histones of lower concentrations were equally efficient in unpacking of the DNA cargo.

Live and Dead Assay. The gene of interest taken here was p53, and its expression leads to the occurrence of apoptosis. In this assay, live cells were stained green and dead cells were stained red. From Figure 11 it was observed that occurrence of cell apoptosis was time dependent based on the incubation time of C6 cells with nanoplexes prepared using Dex-H and p53 plasmid DNA in the ratio 2:1. Significant cell death was detected at the end of 24 h of incubation. The live/dead assay analysis depicted cell membrane permeability due to cell death. The cell population that underwent plasma membrane rupture increased to around 90% at the end of 48 h.

Cytotoxicity Assay of Inhibitors. MTT assay was used to determine the cytotoxicity of controls such as inhibitors and inhibitors with derivative alone which were used to study the endocytic trafficking of Dex-H in the C6 cell line. All the inhibitors depicted % cell viability in the range of 95% to 81% as shown in Figure 12. Controls including Dex-H in the presence of various inhibitors were also checked. It also showed % cell viability in the range of 93% to 79%. Cytotoxicity was detected to be significantly low in the presence of both the controls, proving Dex-H to be nontoxic and that the data obtained on endocytic trafficking is reliable with no toxicity interference by the presence of inhibitors. Results were expressed as means ± standard deviation.

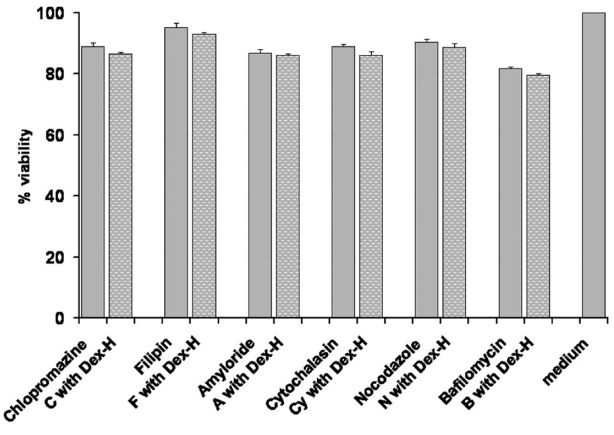

Figure 12. Cytotoxicity of C6 cells after incubation of Dex-H with various inhibitors. Cytotoxicity was evaluated by the MTT assay and expressed as % cell viability. Results are expressed as means ± standard deviation.

Inhibition Assay by Endocytic Inhibitors. To understand the endocytic pathway followed by Dex-H, selective endocytic inhibitors were used to inhibit the endocytosis process. Endocytosis inhibitors have been used to qualitatively assess the role of endocytic pathway to the internalization of nonviral gene delivery systems. Figure 13 shows cell uptake profile of DHP in the presence of endocytic inhibitors.

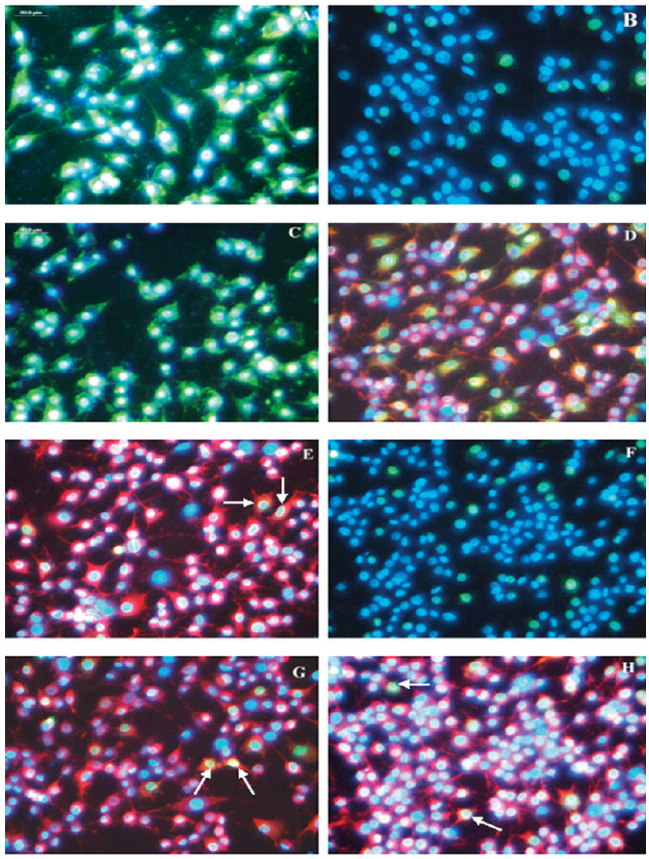

Figure 13. Fluorescence micrographs of C6 cells transfected with Dex-H/DNA complexes in ratio 2:1 in the absence and presence of various endocytic inhibitors individually and in combination. Cells were pretreated with inhibitors for 30 min prior to the experiment and were then incubated with Dex-H/DNA complexes in ratio 2:1 at 37 °C for 3 h under 5% CO_2 atm. Plasmid DNA was tagged with YOYO-I (green). Nucleus was stained using Hoechst 33342 (blue). Actin filaments were stained using TRITC (red). Magnification and scale bar represent 40× and 20 μm respectively. (A) Uninhibited cells. (B) Chlorpromazine treated cells. (C) Filipin treated cells. (D) Amyloride treated cells. (E) Cytochalasin B treated cells. (F) Chlorpromazine and filipin treated cells. (G) Nocodazole and amyloride treated cells. (H) Nocodazole and cytochalasin B treated cells. Arrows depict C6 cells where internalization of Dex-H/DNA complexes has taken place.

Nanoplexes in the absence of inhibitors showed increased gene expression (Figure 13A). The inhibition of the internalization of nanoplexes of Dex-H and plasmid DNA by chlorpromazine, inhibitor of clathrin mediated endocytosis, was found to be more effective (Figure 13B). Increased uptake of nanoplexes was detected in cells treated with filipin, inhibitor of caveolae mediated endocytosis (Figure 13C). Treatment of cells with both chlorpromazine and filipin showed marginal reduction compared to untreated cells (Figure 13F) whereas no much significant change was observed in the presence of amiloride (Figure 13D). On treatment with cytochalasin B, a significant reduction was seen in plasmid assisted fluorescence (Figure 13E). No deleterious effects were seen on the cells in the presence of inhibitors. Marginal decrease of fluorescence was detected in cells treated with both nocodazole and amiloride (Figure 13G). Cells on treatment with both nocodazole and cytochalasin B showed notable reduction of fluorescence by plasmid in the cells (Figure 13H). The above results suggest that DHP depends on both clathrin mediated endocytosis and macropinocytosis for its internalization.

Cells were also treated with bafilomycin A_1, an inhibitor of vacuolar ATPase endosomal proton pump that prevents the acidification of endosomes, to confirm the major role played by imidazole of Dex-H in the success of gene delivery.

On treatment with bafilomycin A_1, plasmid assisted fluorescence was found to diminish significantly. Bafilomycin A_1 inhibits the protonation of imidazole ring, which thus prevents the escape of complexes from the endosome, thereby reducing gene expression as shown in Figure 14.

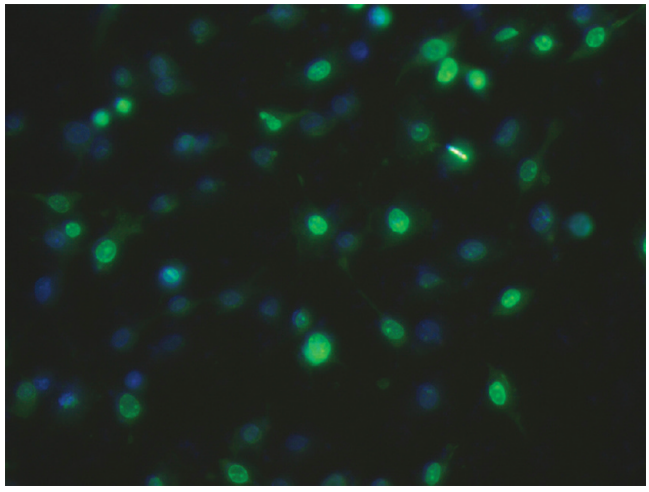

Figure 14. Fluorescence micrographs of C6 cells transfected with Dex-H/DNA complexes in ratio 2:1 in the presence of bafilomycin A1. Cells were pretreated with bafilomycin A1 for 30 min prior to the experiment and were then incubated with Dex-H/DNA complexes in ratio 2:1 at 37 °C for 3 h under 5% CO_2 atm. Plasmid DNA was tagged with YOYO-I (green). Nucleus was stained using Hoechst 33342 (blue). Magnification and scale bar represent 40× and 20 μm respectively.

Inhibition Assay by in Vitro Transfection. Transfection studies were conducted in C6 cells to examine the effect of inhibitors on the cellular uptake of nanoplexes of Dex-H and plasmid DNA. Chlorpromazine reduced transfection efficiency. But in the case of filipin, high reporter gene expression was detected. Moderate luciferase activity was also seen in the presence of nocodazole. Comparison of the transfection efficiencies of the nanoplexes in the presence of selective endocytic inhibitors is shown in Figure 15. Increase in transfection efficiency proves efficient internalization of the nanoplexes by clathrin and macropinocytosis.

Role of Actin and Microtubules. Cells were incubated with nocodazole, and both uptake and transfection were determined using fluorescence microscopy to ascertain the role of microtubules and actin in the internalization of the nanoplexes. The use of TRITC enabled the visualization of actin filaments associated with the plasma membrane. Disrupted actin filaments were detected in the presence of cytochalasin B. In line with the transfection efficiency of the nanoplex, there was however significant effect on the cellular uptake of the nanoplex using the microtubule disrupting agent nocodazole and actin depolymerizing agent cytochalasin B. Figure 13 shows that internalization depends on ruffling of the

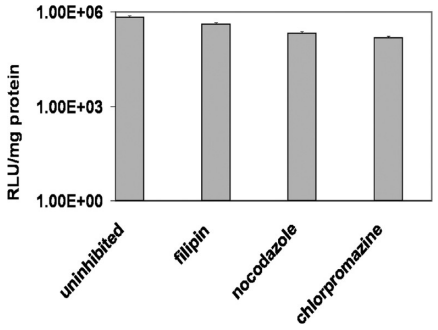

Figure 15. Effect of various endocytic inhibitors on luciferase gene expression of C6 cells. Cells were pretreated with inhibitors for 30 min at 37 °C prior to the experiment and incubated with Dex-H/DNA complexes of weight ratio 2:1 at 37 °C for 3 h under 5% CO_2 atmosphere. In vitro transfection efficiency of Dex-H/DNA complexes in C6 cells in the absence and presence of various endocytic inhibitors (filipin (5 μg/mL), chlorpromazine (2 μg/mL) and nocodazole (7.5 μg/mL)) were evaluated and expressed as relative light units/mg of total cell protein. Results were expressed as means ± standard deviation.

plasma membrane driven by the actin cytoskeleton which has been ascertained by the luciferase activity assay.

■ DISCUSSION

The requirement of a capable gene delivery system is to perform multiple functions at the appropriate time from complexation with the nucleic acid until its expression within the cell. Several barriers pose a problem during the designing of an efficient gene delivery vehicle.

We synthesized a dextran derivative Dex-H by conjugating dextran with histidine moieties so as to obtain an efficient gene delivery system. This can be made possible by utilizing the unique characteristics of imidazole present in histidine. Modification by histidine enables fine-tuning of the properties of dextran required for efficient gene delivery. Periodate oxidation was the preferred method used for conjugation of histidine to dextran. A diamino PEG spacer arm was coupled to dextran so as to incorporate significant histidine residues.

The derivatization of dextran with histidine was confirmed by studying the absorption bands characteristic of Dex-H by FTIR spectroscopy. Major attention was focused on characterizing the occurrence of peaks at 1608.9 cm^{-1} and 1451.6 cm^{-1} which was due to the presence of amide bond. The reaction of dextran with histidine led to the formation of a peak characteristic for imidazole rings at 1091.8 cm^{-1}.

The modification of dextran with histidine was confirmed by NMR spectral studies. It exhibited peaks originating from imidazole at 7.61 ppm and 6.92 ppm, α $-CH-$ peak of histidine at 4.69 ppm and β $-CH_2-$ peak at 2.96 ascertaining the successful derivatization of dextran with histidine.

The spectrophotometric analysis of the histidine moieties on dextran by the use of sulfanilic acid inferred that 32.4 mg of histidine was found bound to 1 g of dextran.

The molecular weight of dextran used for synthesizing the derivative was 35,600 Da. The molecular weight of the derivative was experimentally detected to be 36,982 Da. This was detected to be in accord with the spectrophotometric analysis of the histidine moieties by the use of sulfanilic acid. The molecular weights between the parent polymer and the derivative showed no significant difference, thus also proving that the approach used in synthesizing the derivative did not result in cross-linking of the polymers.

The first barrier in gene delivery is the condensation of DNA by the cationic polymer into nanometric sized nanoplexes which is less than 150 nm to allow cellular internalization.[29] In vitro transfection encounters several negatively charged barriers like serum proteins and cell membranes which if overcome would facilitate successful gene delivery. Cationic polymers electrostatically interact with the anionic cell membrane.[30,31] While designing a nucleic acid carrier, one must keep in mind that, for efficient nucleic acid delivery, nanoparticles should bear a positive surface charge. Dex-H of the optimum ratio of 2:1 exhibited a positive zeta potential value of +10 mV.

Understanding different surface properties is crucial while formulating nucleic acid delivery vectors as they influence cellular uptake and distribution. From the molecular topography of plasmid DNA, it was clear that DNA could easily be compacted into nanometric sized complexes on complexation with cationic polymers. The condensation of DNA into small complexes can facilitate its easy entry into the cell.[32] The condensation of DNA with cationic Dex-H to form DHP by electrostatic interactions ensures encapsulation and protection of the plasmid from enzymatic degradation.[33] The smallest complex of size 112 nm was formed by the Dex-H/DNA complex at a weight ratio of 2:1.

The predominant role of Dex-H is to be chemically stable for long so as to protect the nanoplex all the way to the nucleus, and it should also be able to escape the endosomal compartment and release DNA into the nucleus. A strong cationic nanoplex is formed by the electrostatic interactions between Dex-H and ctDNA. The gel retardation assay confirmed the strength of complexation of ctDNA with Dex-H. In the presence of EtBr, nucleic acids fluoresce due to the intercalation of the dye with the minor groove of DNA helix.[34] As the concentration of Dex-H increased, ctDNA gradually lost its mobility due to the increase in the shielding effect of the polymer. Lower DNA binding capability was detected in Dex-H/ctDNA nanoplexes at weight ratios less than 2:1. The strong electrostatic interaction between the polymer and ctDNA thus caused the retardation of DNA in the agarose well.[35] Strong anionic agents were believed to elute out the DNA from the complexes if the polymer was loosely bound to the DNA. The heparin release studies confirmed the strong complexation of DNA with Dex-H, and thus heparin, being an anionic agent, was not able to displace DNA from Dex-H.

Binding affinity of Dex-H to plasmid DNA was checked by complexing Dex-H with p53 plasmid DNA. Strong complexation was detected. Plasmid DNA exists in a nonlinear state as compared to ctDNA. Polymer binds tightly with the plasmid DNA such that even the fluorescence of EtBr intercalated with the plasmid DNA is unseen. The experiment also inferred that heparin does not release the plasmid DNA from the strongly bound complex.

The second barrier is the ability of the delivery vehicle to enhance its escape from the endosome rather than being transferred to lysosomes for degradation.[36] The nanoplex after endosomal uptake by the cell has to escape from the endosome to prevent its own lysosomal degradation. This can be made possible based on the hypothesis for endosomal escape called the "proton sponge theory" which focuses on the escape of the nanoplexes from the endosomes by their acidification. This brings about large differences in the surface charge of the nanoplex, which leads to structural changes. Disruption of the interaction between the nanoplex and the endosomal membrane is thus caused, which is followed by their escape

from the endosome.[36,37] Studies have been conducted where histidine polymers have been found to have DNA condensing properties, good transfection capability and endosomolytic properties.[38,39] The pK_a of imidazole in histidine being around 6.0 specifies the protonation of the polymer and its existence as a strong polycation over the entire endosomal pH range. Dex-H, whose principal component is histidine, exhibited a very high buffering capacity at two different concentrations of 20 μg/mL and 40 μg/mL in the pH range of 10 to 6 due to the higher concentrations of imidazole rings. This proves the capability of Dex-H as an efficient gene vector as it enhances its escape from the endosome and thus brings about higher gene expression.

The third barrier is the need to target the gene vector to specific cell types efficiently and to release the plasmid DNA into the cell cytoplasm with minimal toxicity. This is determined by the efficacy of transfection and cytotoxicity.[40]

Cytotoxicity was inferred to be due to the interaction of the cationic polymer with either the plasma membrane or cell components.[41] Reduction in cellular metabolic activity denotes cell injury. In vitro cytotoxicity of Dex-H at various concentrations ranging from 25 μg/mL to 5 mg/mL was assessed on C6 cells and HepG2 cells using MTT assay. Dex-H ascertained minimal cytotoxic nature even at a higher concentration of 5 mg/mL in both the cell lines. The cytotoxic potential of the polymer significantly reduced as the concentration of Dex-H decreased. This was speculated to be due to the counterbalance of the negative charge of DNA with the positive charge of Dex-H, which thus minimized the interactions with cell membrane. Even though dextran may have an inherently low cytotoxic profile, the subsistence of histidine helped Dex-H to have reduced polymer cytotoxicity as proved from cell studies.

One of the major factors impeding transfection efficacies is release of plasmid DNA by the vector after cell entry into the cell cytoplasm. Earlier reports have shown that improved transfection efficacies with minimal toxic effects have been achieved by modification of the architecture of polymers using endosome disrupting histidine functionalities.[42,43] Transfection by Dex-H, in comparison with PEI, depicted a considerably high level of gene expression in three ratios depicted. The strong complexation of Dex-H with plasmid DNA provided the polymer favorable transfection efficiency at a lower ratio of 2:1 in both C6 and HepG2 cell lines. In the presence of 10% FBS, the efficiency of transfection was found to enhance for all the ratios investigated. Transfecting cells have several advantages in the presence of serum, like less time consumption, easy transfections, low experimental cost and avoidance of the cell's deprivation of serum.[1] Enhancement of gene transfection efficiency by Dex-H was assumed to be due to the destabilization of endosomal membranes by histidine moieties.[42,44,45]

The fourth barrier is the capability of the gene vector to unpack its DNA cargo, translocate the DNA into the nucleus and bring forth the expression of the gene.[46]

The major factor governing an efficient gene delivery vector is its capability to successfully deliver the gene into the host cell nucleus and to induce gene expression for longer periods of time. The cellular uptake of the plasmid was visualized by fluorescently labeling using YOYO-I and was tracked using the fluorescent microscope. When DHP were monitored, plasmid DNA was found localized in the nucleus of the cells and diffused in the cytoplasmic area. This was found in accord with the presence of histidine moieties in Dex-H, which helped in the increase of nuclear access of DNA by its endosomolytic behavior.

The efficiency of cellular uptake by the polymer was visualized by fluorescently labeling Dex-H with TRITC and was tracked using a fluorescence microscope. Intense fluorescence of Dex-H was seen within the cell, indicating strong interaction of the polymer with the cell membrane. Dex-H remained in the cytoplasm and did not enter into the nucleus. From the above trafficking results, it appeared that, following the escape of the nanoplexes from the endosome, DNA detaches from Dex-H and enters into the nucleus.

For the occurrence of proper transfection, excessive cellular uptake is necessary as endosomal escape and intracellular trafficking block the expression of the plasmid entered. High gene expression followed by efficient cellular internalization is of real concern, which reinforces the need of a molecule which helps in unpacking of DNA from the carrier, such as histone. In this study, Dex-H was determined to be a remarkable transfecting agent which efficiently transports the nanoplex into the cell by endocytosis and allows its safe entry into the cytoplasm by escaping from the endosome. The polymer was then found to unpack its cargo DNA for its entry into the nucleus and gene expression. The unpacking of DNA from its polymer was hypothesized to be performed by histones. This was proved by the experiment performed in vitro in the presence and absence of histones. The internalization capability of Dex-H and plasmid was monitored by tagging both the polymer and DNA with fluorescent tags. In the absence of histone, presence of polymer was detected in the cytoplasm and DNA in the nucleus. The entry of Dex-H (red) detected in the cytoplasm and near the nucleus confirmed its efficiency as a delivery vector. At the end of 3 h incubation of C6 cells with fluorescently labeled DHP, in the presence of histone, only fluorescent signals from DNA (green) were found to be intense inside the nuclear region and dispersed evenly in the cytoplasmic region. Lack of fluorescence signals from the polymer depicted the complete dissociation of the polymer from DNA on incubation with histone. Here, the unpacking of the DNA from the polymer by histones took place outside the cell itself and thus no polymer was detected anywhere in the cell after the cell uptake. This proved that histones were responsible for unpacking DNA from the polymer in the cell as seen in the experiment performed in the absence of histones from incubation with the nanoplex. The unpacking of DNA from the polymer led to the tight association of DNA with histone resulting in efficient delivery of the gene. This was applicable to a range of histone concentrations varying from 80 μg to 1 ng. Becker et al. also proved the rapid entry of histones into tumor cells which provided strong support to the successful cellular entry when conjugated with histones.[47] Thus it was hypothesized that the DNA and polymer remained tightly associated until it reached the cytoplasm and then the DNA was unpacked and transported into the nucleus as detected by YOYO labeling. Here polymer stayed back in the cytoplasm as detected by TRITC labeling. The significance of this observation is that it can be hypothesized that the histones do play a role in vector unpacking in the cytoplasm. Another advantage may be that by developing polymers with optimum affinity to DNA, with respect to histone, will ensure the unpacking in the cytoplasm leading to enhanced transfection efficiency.

In this study, the prolonged evaluation of gene expression by p53 gene internalized with the help of Dex-H was examined.

The efficacy of the polymer in delivering the transgene into the cell was proved by visualizing the expression of the transgene as apoptosis. The successful transfection of p53 gene into C6 cells was determined by the activation of the apoptosis process. Live cells were stained green, and dead cells were stained red. The morphology of the transfected cells was observed to investigate the apoptotic behavior of the cells. Cells transfected with DHP began to show the expression of p53 gene after 24 h, indicating successful gene delivery into the nucleus. Cell death was found to be time dependent. At the end of 48 h, the cell population that underwent plasma membrane rupture increased to around 90%. So the right delivery of the gene by the polymer into the cell in a significant amount led to its expression which when detected proved the capability of Dex-H as an efficient gene delivery vector.

The fifth barrier is the specific route of entry of the delivery vehicle into the cell. A delivery vector that has precise control over the route of its entry into the cells would be an ideal system for in vivo applications. Cellular uptake involves several types of endocytosis based on cell type, type of vectors and surface properties like size and surface charge.[48] The capability of DHP to use distinctly different entry portals was investigated using inhibitors of endocytic entry pathways. The inhibitors were used at nontoxic concentrations. This was determined by the MTT assay wherein the viability levels of all the inhibitors was above 80%. Controls including Dex-H in the presence of various inhibitors were also checked, proving Dex-H to be nontoxic in the presence of inhibitors. The abolishment of DNA activity and DNA assisted fluorescence in cells treated with endocytic inhibitors affirms the internalization of DHP through an endocytic pathway.[49,50]

Chlorpromazine inhibits clathrin mediated endocytosis by triggering the loss of clathrin from the cell surface.[51] Filipin inhibited caveolae mediated endocytosis.[52] When cells were treated with chlorpromazine, uptake by the cells was found to be reduced. But in the case of cells treated with filipin, the number of fluorescent cells increased. The treatment of cells with both inhibitors together showed an increase in the inhibition of the DHP uptake. Enrichment of plasmid in the nuclear region was detected both in untreated cells and in those treated with filipin respectively. The above results suggest that DHP depends on clathrin mediated endocytosis for its uptake. Reports demonstrated that filipin treatment did not affect macropinocytosis in rat fibroblasts.[53] Macropinocytosis involves uptake by the actin driven ruffling of plasma membrane whereas long-range transport of macropinosomes are favored by microtubules. Thus actin and microtubules are known criteria for macropinocytosis, which is the major route for positively charged complexes.[54] Amiloride inhibits macropinocytosis by inhibiting the sodium proton exchange. There was not much effect on the internalization of DHP with amiloride. We indeed did observe a slight decrease of fluorescence in cells treated with both nocodazole and amiloride.

Binding of nonviral cationic vectors to actin network is a general means to be engulfed into the cell.[28] Cells were also treated with nocodazole and cytochalasin B to identify the role of microtubules and actin in the uptake mechanism respectively. Studies have shown the occurrence of endocytosis at the plasma membrane, which has a direct link with the actin cytoskeleton. Cytochalasin B blocks actin polymerization[55] whereas nocodazole depolymerizes microtubules. In the presence of cytochalasin B, disrupted actin filaments were seen along with loss of fluorescence related to the uptake of DHP. Cells on treatment with both nocodazole and cytochalasin B showed notable reduction of fluorescence by plasmid in the cells. This called forth for the consideration of macropinocytosis in the uptake mechanism. This states the fact that DHP enters the cells by more than one pathway.

It has been inferred that clathrin mediated endocytosis utilizes the actin cytoskeleton to serve its purpose.[56] Our findings denote a direct link between the entry of DHP and actin filaments and microtubules in C6 cells. We were able to detect the significant inhibition of DHP uptake following actin polymerization using cytochalasin B.

These results were consistent with the transfection efficiency obtained with several endocytic inhibitors. A significant decrease was detected in the presence of chlorpromazine whereas a dramatic increase was found in the presence of filipin. While chlorpromazine significantly reduces the uptake of DHP, it is reasonable to presume that uptake mainly depends on clathrin mediated mechanism. It has been reported that particles with a size limit of 150 nm are generally accepted for cellular uptake by clathrin mediated endocytosis, which was in correlation to the size of DHP obtained.[57] From literature, clathrin meditated endocytosis has been found to lead polyplexes to lysosomal degradation. This has been avoided by the high buffering capacity of Dex-H which helps the nanoplexes to escape from the endosome before it fuses with the lysosome.[58] Thus, the uptake of DHP was inhibited by chlorpromazine, nocodazole and cytochalasin B but was not affected by amiloride and filipin. It was also found that the uptake was downregulated by all four inhibitors. This was in accordance with the transfection efficiency evaluated. Transfection was abolished only in the case of chlorpromazine, nocodazole and cytochalasin B. The above predictions implicate both clathrin mediated endocytosis and macropinocytosis as the precise route of DHP internalization. Gene expression was also found to be diminished significantly in the presence of bafilomycin A_1. This is due to the inhibition of the protonation of imidazole ring, which thus prevents the escape of complexes from the endosome thereby reducing gene expression. This reduction also signifies the requirement of endosomal acidification for a successful gene delivery. The derivative Dex-H prepared was found to have remarkable buffering capacity due to the presence of histidine. The high transfection efficiency and reduction in gene expression in the presence of bafilomycin A_1 confirms the escape of the complexes from the endosome before the interaction with lysosome which leads to its degradation.

The above investigations prove that our designed polymer named Dex-H, which incorporates both dextran and histidine, exhibits several attractive properties as a nonviral system. The formulated polymer/DNA complex prepared was of nanometric size, which aided in high cell uptake. They showed remarkable transfection efficiency with minimal cytotoxic effects. It also leads to efficient delivery of the gene into the nucleus and significant expression of the transgene based on the proton sponge effect. This system is efficient in vector unpacking wherein the polymer gets displaced from its DNA cargo and is efficiently taken into the nucleus with the help of histones.

In short, this system (Dex-H) can perform multiple tasks like condense DNA for easy cell migration, endocytose the vector, protect DNA from degradation, escape from the endosomal compartment, shield against undesired interactions, unpack the

vector, enhance cell binding and cellular uptake, translocate DNA into the nucleus, and express the transgene significantly.

■ ASSOCIATED CONTENT

Supporting Information

FTIR spectra of dextran and of Dex-H. Table of zeta potential, hydrodynamic diameter and polydispersity index of Dex-H−DNA complexes at different weight ratios measured after 30 min of incubation. Stability of Dex-H/p53 plasmid DNA complexes at different weight ratios detected after 30 min of incubation in the presence and absence of heparin compared with naked DNA. This material is available free of charge via the Internet at http://pubs.acs.org.

■ AUTHOR INFORMATION

Corresponding Author

*C.P.S.: Biosurface Technology Division, Biomedical Technology Wing, Sree Chitra Tirunal Institute for Medical Sciences & Technology, Thiruvananthapuram, Kerala, India; tel, 91-471-2520214; fax, 91-471-2341814; e-mail, sharmacp@sctimst.ac.in. M.R.R.: Scientist, Biosurface Technology Division Biomedical Technology Wing, Sree Chitra Tirunal Institute for Medical Sciences & Technology Thiruvananthapuram, Kerala, India; tel, 91-471-2520284; fax, 91-471-2341814; e-mail, rekhamr@sctimst.ac.in.

■ ACKNOWLEDGMENTS

We express our sincere thanks to The Director, SCTIMST and The Head, BMT Wing for the facilities provided. Authors are thankful to the financial support from FADDS, DST, New Delhi. One of the authors (C.P.S.) expresses his thanks to Prof. Allan S. Hoffman, University of Washington, Seattle, WA, United States, for directing the attention to the role of histones in gene delivery. The authors thank Dr. H. K Varma, SCTIMST for the FTIR facility.

■ REFERENCES

(1) Choi, S.; Lee, K. D. Enhanced gene delivery using disulfide-crosslinked low molecular weight polyethylenimine with listeriolysin o-polyethylenimine disulfide conjugate. *J. Controlled Release* **2008**, *131*, 70−76.

(2) Smith, A. E. Viral vectors in gene therapy. *Annu. Rev. Microbiol.* **1995**, *49*, 807−838.

(3) Kim, T. H.; Park, I. K.; Kim, S. I.; Jeong, H. J.; Bom, H. S.; Cho, C. S. Chitosan Derivatives as Gene Carriers. *Key Eng. Mater.* **2005**, *288*−*289*, 97−100.

(4) Hosseinkhani, H.; Azzam, T.; Tabata, Y.; Domb, A. J. Dextran-spermine polycation: an efficient non-viral vector for in vitro and in vivo gene transfection. *Gene Ther.* **2004**, *11*, 194−203.

(5) Cavallaro, G.; Scirè, S.; Licciardi, M.; Ogris, M.; Wagner, E.; Giammona, G. Polyhydroxyethylaspartamide-spermine copolymers: Efficient vectors for gene delivery. *J. Controlled Release* **2008**, *131*, 54−63.

(6) Tsuchiya, Y.; Ishii, T.; Okahata, Y.; Sato, T. Characterization of Protamine as a Transfection Accelerator for Gene Delivery. *J. Bioact. Compat. Polym.* **2006**, *21*, 519−537.

(7) Thomas, J. J.; Rekha, M. R.; Sharma, C. P. Dextran glycidyltrimethylammonium chloride conjugate/DNA nanoples: A potential non-viral and haemocompatible gene delivery system. *Int. J. Pharm.* **2010**, *389*, 195−206.

(8) Yalpani, M.; Hedman, P. O. Preparation and applications of dextran-derived products in biotechnology and related areas. *Crit. Rev. Biotechnol.* **1985**, *3*, 375−421.

(9) Thomas, J. J.; Rekha, M. R.; Sharma, C. P. Dextran-protamine polycation: An efficient nonviral and haemocompatible gene delivery system. *Colloids Surf. B* **2010**, *81*, 195−205.

(10) Vroman, B.; Ferreira, I.; Jerome, C.; Jerome, R.; Preat, V. PEGylated quaternized copolymer/DNA complexes for gene delivery. *Int. J. Pharm.* **2007**, *34*, 88−95.

(11) Laemmli, U. K. Characterization of DNA condensates induced by poly(ethylene oxide) and polylysine. *Proc. Natl. Acad. Sci. U.S.A.* **1975**, *72*, 4288−4292.

(12) Demberelnyamba, D.; Kim, K. S.; Choi, S.; Park, S. Y.; Lee, H.; Kim, C. J.; Yoo, I. D. Synthesis and antimicrobial properties of imidazolium and pyrrolidinonium salts. *Bioorg. Med. Chem.* **2004**, *12*, 853−857.

(13) Bando, T.; Sugiyama, H. Synthesis and Biological Properties of Sequence-Specific DNA-Alkylating Pyrrole-Imidazole Polyamides. *Acc. Chem. Res.* **2006**, *39*, 935−944.

(14) De Luca, L. Naturally Occurring and Synthetic Imidazoles: Their Chemistry and Their Biological Activities. *Curr. Med. Chem.* **2006**, *13*, 1−13.

(15) Hofmann, K. *The chemistry of heterocyclic compounds, imidazole and derivatives part 1*; Interscience Publishers, Inc.: New York, 1953.

(16) Grimmett, M. R. *Imidazole and benzimidazole synthesis*; Academic Press, Inc.: 1997.

(17) Gava, B.; Zorzet., S.; Spessotto, P.; Cocchietto, M.; Sava, G. Inhibition of B16 Melanoma Metastases with the Ruthenium Complex Imidazolium trans-Imidazoledimethylsulfoxide-tetrachlororuthenate and Down-Regulation of Tumor Cell Invasion. *J. Pharmacol. Exp. Ther.* **2006**, *317*, 284−291.

(18) Frade, R. F. M.; Rosatella, A. A.; Marques, C. S.; Branco, L. C.; Kulkarni, P. S.; Mateus, N. M. M.; Afonso, C. A. M.; Duarte, C. M. M. Toxicological evaluation on human colon carcinoma cell line (CaCo-2) of ionic liquids based on imidazolium, guanidinium, ammonium, phosphonium, pyridinium and pyrrolidinium cations. *Green Chem.* **2009**, *11*, 1660−1665.

(19) Zhang, C.; Ding, Z.; Suhaimi, N. M.; Kng, Y. L.; Zhang, Y.; Zhuo, L. A class of imidazolium salts is anti-oxidative and anti-fibrotic in hepatic stellate cells. *Free Radical Res.* **2009**, *43*, 899−912.

(20) Behr, J. The proton sponge: a trick to enter cells the viruses did not exploit. *Chimia* **1997**, *51*, 34−36.

(21) Richardson, S.; Ferruti, P.; Duncan, R. Poly(amidoamine)s as potential endosomolytic polymers: evaluation in vitro and body distribution in normal and tumour-bearing animals. *J. Drug Targeting* **1999**, *6*, 391−404.

(22) Akinc, A.; Thomas, M.; Klibanov, A. M.; Langer, R. Exploring polyethylenimine-mediated DNA transfection and the proton sponge hypothesis. *J. Gene Med.* **2005**, *7*, 657−63.

(23) Kichler, A.; Leborgne, C.; März, J.; Danos, O.; Bechinger, B. Histidine-rich amphipathic peptide antibiotics promote efficient delivery of DNA into mammalian cells. *Proc. Natl. Acad. Sci. U.S.A.* **2003**, *96*, 1564−1568.

(24) Kichler, A.; Mason, A. J.; Bechinger, B. Cationic amphipathic histidine- rich peptides for gene delivery. *Biochim. Biophys. Acta* **2006**, *1758*, 301−307.

(25) Park, J. S.; Han, T. H.; Lee, K. Y.; Han, S. S.; Hwang, J. J.; Moon, D. H.; Kim, S. Y.; Cho, Y. W. N-acetyl histidine-conjugated glycol chitosan self-assembled nanoparticles for intracytoplasmic delivery of drugs: Endocytosis, exocytosis and drug release. *J. Controlled Release* **2006**, *115*, 37−45.

(26) Azzam, T.; Eliyahu, H.; Shapira, L.; Linial, M.; Barenholz, Y.; Domb, A. J. Polysaccharide-oligoamine based conjugates for gene delivery. *J. Med. Chem.* **2002**, *45*, 1817−1824.

(27) Vandana, P.; Kalpesh, P.; Mukund, S.; Mayank, B. Spectrophotometric Determination of Histidine Hydrochloride Monohydrate in Pharmaceutical Formulations. *Int. J. PharmTech Res.* **2009**, *1*, 852−856.

(28) Kanatani, I.; Ikai, T.; Okazaki, A.; Jo, J.; Yamamoto, M.; Imamura, M.; Kanematsu, A.; Yamamoto, S.; Ito, N.; Ogawa, O.; Tabata, Y. Efficient gene transfer by pullulan−spermine occurs

through both clathrin- and raft/caveolae-dependent mechanisms. *J. Controlled Release* **2006**, *116*, 75−82.
(29) Putnam, D.; Gentry, C. A.; Pack, D. W.; Langer, R. Polymer-based gene delivery with low cytotoxicity by a unique balance of side-chain termini. *Proc. Natl. Acad. Sci. U.S.A.* **2001**, *98*, 1200−1205.
(30) Blau, S.; Jubeh, T. T.; Haupt, S. M.; Rubinstein, A. Drug targeting by surface cationization. *Crit. Rev. Ther. Drug Carrier Syst.* **2000**, *17*, 425−465.
(31) Kim, T.; Baek, J.; Yoon, J. K.; Choi, J. S.; Kim, K.; Park, J. S. Synthesis and characterization of a novel arginine-grafted dendritic block copolymer for gene delivery and study of its cellular uptake pathway leading to transfection. *Bioconjugate Chem.* **2007**, *18*, 309−317.
(32) Lin, C.; Zhong, Z. Y.; Lok, M. C.; Jiang, X. L.; Hennink, W. E.; Feijen, J.; Engbersen, J. F. J. Linear poly (amidoamine)s with secondary and tertiary amino groups and variable amounts of disulphide linkages: synthesis and invitro gene transfer properties. *J. Controlled Release* **2006**, *116*, 130−137.
(33) Burckbuchler, V.; Wintgens, V.; Lecomte, S.; Percot, A.; Leborgne, C.; Danos, O.; Kichler, A.; Amiel, C. DNA compaction into new DNA vectors based on cyclodextrin polymer: surface enhanced Raman spectroscopy characterization. *Biopolymers* **2006**, *81*, 360−370.
(34) Warning, M. J. Complex formation between ethidium bromide and nucleic acids. *J. Mol. Biol.* **1965**, *13*, 269−282.
(35) Wolfert, M. A.; Schacht, E. H.; Toncheva, V.; Ulbrich, K.; Nazarova, O.; Seymour, L. W. Characterization of vectors for gene therapy formed by self-assembly of DNA with synthetic block co-polymers. *Hum. Gene Ther.* **1996**, *7*, 2123−2133.
(36) Midoux, P.; Kichler, A.; Boutin, V.; Maurizot, J. C.; Monsigny, M. Membrane permeabilization and efficient gene transfer by a peptide containing several histidines. *Bioconjugate Chem.* **1998**, *9*, 260−267.
(37) Akinc, A.; Thomas, M.; Klibanov, A. M.; Langer, R. Exploring polyethylenimine mediated DNA transfection and the proton sponge hypothesis. *J. Gene Med.* **2005**, *7*, 657−663.
(38) Tang, M. X.; Szoka, F. C. The influence of polymer structure on the interactions of cationic polymers with DNA and morphology of the resulting complexes. *Gene Ther.* **1997**, *4*, 823−832.
(39) Wang, C. Y.; Huang, L. (1984) Polyhistidine mediates an acid-dependent fusion of negatively charged liposomes. *Biochemistry* **1984**, *23*, 4409−4416.
(40) Benns, J. M.; Kim, S. W. Tailoring New Gene Delivery Designs for Specific Targets. *J. Drug Targeting* **2000**, *8*, 1−12.
(41) Fischer, D.; Li, Y. X.; Ahlemeyer, B.; Krieglstein, J.; Kissel, T. In vitro cytotoxicity testing of polycations: influence of polymer structure on cell viability and haemolysis. *Biomaterials* **2003**, *24*, 1121−1131.
(42) Midoux, P.; Monsigny, M. Efficient gene transfer by histidylated polylysine /pDNA complexes. *Bioconjugate Chem.* **1999**, *10*, 406−411.
(43) Pichon, C.; Roufa, M. B.; Monsigny, M.; Midoux, P. Histidylated oligolysines increase the transmembrane passage and the biological activity of antisense oligonucleotides. *Nucleic Acids Res.* **2000**, *28*, 504−512.
(44) Roufai, M. B.; Midoux, P. Histidylated polylysine as DNA vector: elevation of the imidazole protonation and reduced cellular uptake without change in the polyfection efficiency of serum negative polyplexes. *Bioconjugate Chem.* **2001**, *12*, 92−99.
(45) Pack, D. W.; Putnam, D.; Langer, R. (2000) Design of imidazole-containing endosomolytic biopolymers for gene delivery. *Biotechnol. Bioeng.* **2000**, *6*, 217−223.
(46) Zanta, M. A.; Belguise-Valladier, P.; Behr, J. P. Gene delivery: a single nuclear localization signal peptide is sufficient to carry DNA to the cell nucleus. *Proc. Natl. Acad. Sci. U.S.A.* **1999**, *96*, 91−96.
(47) Becker, F. F.; Green, H. Effect of protamines and histones on the nucleic acids of ascites tumor cells. *Exp. Cell Res.* **1960**, *19*, 361−375.
(48) Wattiaux, R.; Laurent, N.; Wattiaux-De Coninck, S.; Jadot, M. Endosomes, lysosomes: their implication in gene transfer. *Adv. Drug Delivery Rev.* **2000**, *41*, 201−208.
(49) Boussif, O.; Lezoualc'h, F.; Zanta, M. A.; Mergny, M. D.; Scherman, D.; Demeneix, B.; Behr, J. P. A versatile vector for gene and oligonucleotide transfer into cells in culture and in vivo: polyethyleneimine. *Proc. Natl. Acad. Sci. U.S.A.* **1995**, *92*, 7297−7301.
(50) Godbey, W. T.; Wu, K. K.; Mikos, A. G. Tracking the intracellular path of poly(ethylenimine)/DNA complexes for gene delivery. *Proc. Natl. Acad. Sci. U.S.A.* **1999**, *96*, 5177−5181.
(51) Tulapurkara, M. E.; Schäfera, R.; Hancka, T.; Floresb, R. V.; Weismand, G. A.; Gonzálezb, F. A.; Reisera, G. Endocytosis mechanism of P2Y2 nucleotidereceptor tagged with green fluorescent protein: clathrin and actin cytoskeleton dependence. *Cell. Mol. Life Sci.* **2005**, *62*, 1388−1399.
(52) Orlandi, P. A.; Fishman, P. H. Filipin-dependent inhibition of cholera toxin: evidence for toxin internalization and activation through caveolae-like domains. *J. Cell Biol.* **1998**, *141*, 905−915.
(53) Monis, G. F; Schultz, C.; Ren, R.; Eberhard, J.; Costello, C.; Connors, L.; Skinner, M.; Trinkaus-Randall, V. Role of endocytic inhibitory drugs on internalization of amyloidogenic light chains by cardiac fibroblasts. *Am. J. Pathol.* **2006**, *169*, 1939−1952.
(54) Adler, A. F.; Leong, K. W. Emerging links between surface nanotechnology and endocytosis: Impact on nonviral gene delivery. *Nano Today* **2010**, *5*, 553−569.
(55) Peterson, J. R.; Mitchison, T. J. Small molecules, big impact: a history of chemical inhibitors and the cytoskeleton. *Chem. Biol.* **2002**, *9*, 1275−1285.
(56) Da Costa, S. R.; Okamoto, C. T.; Hamm-Alvarez, S. F. Actin microfilaments et al.—the many components, effectors and regulators of epithelial cell endocytosis. *Adv. Drug Delivery Rev.* **2003**, *55*, 1359−1383.
(57) Bishop, N. E. An update on non-clathrin-coated endocytosis. *Rev. Med. Virol.* **1997**, *7*, 199−209.
(58) Panyam, J.; Zhou, W. Z.; Prabha, S.; Sahoo, S. K.; Labhasetwar, V. Rapid endo-lysosomal escape of poly(DL-lactide-co-glycolide) nanoparticles: implications for drug and gene delivery. *FASEB J.* **2002**, *16*, 1217−1226.